Hydrogen-1 Nuclear Magnetic Resonance Investigation of High-Potential Iron–Sulfur Proteins from *Ectothiorhodospira halophila* and *Ectothiorhodospira vacuolata*: A Comparative Study of Hyperfine-Shifted Resonances†

R. Krishnamoorthi and John L. Markley*
Department of Chemistry, Purdue University, West Lafayette, Indiana 47907
Michael A. Cusanovich, C. T. Przysiecki,‡ and T. E. Meyer
Department of Biochemistry, University of Arizona, Tucson, Arizona 85721
Received June 14, 1985

ABSTRACT: Proton NMR spectra of the oxidized and reduced forms of high-potential iron–sulfur proteins (HiPIPs) were recorded at 200 MHz. The proteins studied were the HiPIPs I and II from *Ectothiorhodospira halophila* and *Ectothiorhodospira vacuolata*. Hyperfine-shifted peaks in spectra of the oxidized proteins were assigned to some of the protons of the cysteinyl ligands and aromatic residues at the active site on the basis of their chemical shifts, longitudinal relaxation times, and temperature-dependent behavior. The cysteinyl C_β-H protons were found to resonate downfield (about 100 ppm) and the C_α-H protons upfield (about −25 ppm). This hyperfine shift pattern is consistent with the observed isotropic shift being contact in origin; it probably results from a π-spin-transfer mechanism. The large magnitudes of the chemical shifts of peaks assigned to aromatic residues suggest that these residues interact with the iron–sulfur cluster via π–π overlap. Some of the hyperfine-shifted peaks observed in water were found to disappear in ^2H_2O solution. Such resonances probably arise from exchange-labile hydrogens of amino acid residues directly hydrogen bonded to the iron–sulfur cluster. In the case of HiPIPs I and II from *E. vacuolata*, whose spectra are similar except for the number of such peaks, the relative number of hydrogen bonds inferred to be present in the oxidized and reduced proteins qualitatively explains the difference between their midpoint redox potentials. On the other hand, for *E. halophila* HiPIPs I and II, consideration of the inferred number of hydrogen bonds alone fails to predict the sign of the difference between their midpoint redox potentials. The latter two proteins exhibited different patterns of nonexchangeable hyperfine-shifted peaks with oxidized *E. halophila* HiPIP II having an additional pair of peaks at high field that were attributed to aromatic residues in contact with the iron–sulfur cluster. Such aromatic interactions appear to modulate the redox potential of the active site in these HiPIPs.

High-potential iron–sulfur protein (HiPIP)[1] ($M_r \leq 9000$), found in photosynthetic bacteria, undergoes reversible one-electron-transfer reactions. Its specific functional role in biochemical pathways is unknown; however, *Chromatium vinosum* HiPIP has been found to interact readily with a thiosulfate-oxidizing enzyme isolated from the same bacterium (Fukumari & Yamanaka, 1979). The $(Cys\text{-}S\text{-})_4$–Fe_4S_4 prosthetic group of oxidized HiPIP is paramagnetic with a net negative charge; in the reduced form, it is predominantly diamagnetic, because the two unpaired spins of the cluster are exchange-coupled, resulting in antiferromagnetism (Phillips et al., 1970). A fundamental issue in iron–sulfur protein research is the identification of sources of modulation of the redox potential of a given type of active site. The following two mechanisms have been suggested: (i) polypeptide constraints of the electronic geometry of the iron–sulfur cluster (Carter, 1977b; Carter et al., 1974; Laskowski et al., 1978) and (ii) backbone amide NH···S hydrogen bonds at the active site (Carter, 1977a; Sheridan & Allen, 1980; Sheridan et al., 1981, 1984). While the X-ray crystallographic structure of *C. vinosum* HiPIP (Carter et al., 1974) indicated the presence of several hydrogen bonds between the polypeptide chain and the iron–sulfur cluster, their role as modulators of the redox potential has been little explored (Adman et al., 1975). However, the potential significance of these hydrogen bonds has been deduced from theoretical studies of model compounds (Sheridan et al., 1981, 1984).

Proton NMR spectroscopy is ideally suited for investigating the electronic and molecular structure of the HiPIP active site. The oxidized protein yields well-resolved peaks from the iron ligands and other amino acid residues that are near the iron–sulfur cluster; these signals are shifted far away from the crowded diamagnetic spectral envelope by electron–nuclear hyperfine interactions (Phillips et al., 1970; Phillips & Poe, 1973; Phillips, 1973). In fact, the hyperfine-shifted resonances occur at even higher field (ca. −30 ppm) and lower field (~100 ppm) extremes than observed previously with a HiPIP (Nettesheim et al., 1983). The chemical shifts of these signals

† This research was supported by grants from the U.S. Department of Agriculture Competitive Research Grants Office, Cooperative State Research Service, Science and Education (82-CRCR-1-1045 to J.L.M.), and the National Institutes of Health (GM 21277 to M.A.C.). The Purdue University Biochemical Magnetic Resonance Laboratory has financial support from Grant RR 01077 from Biotechnology Resources, National Institutes of Health.

* Address correspondence to this author at the Department of Biochemistry, University of Wisconsin—Madison, Madison, WI 53706.
‡ Present address: Department of Clinical Pharmacology, Beth Israel Hospital, Boston, MA 02115.

[1] Abbreviations: HiPIP, high-potential iron–sulfur protein; 4Fe-4S, cluster containing four iron atoms and four inorganic sulfur atoms; ppm, parts per million; NMR, nuclear magnetic resonance; NOE, nuclear Overhauser effect; DSS, sodium salt of 4,4-dimethyl-4-silapentane-1-sulfonic acid.

0006-2960/86/0425-0060$01.50/0

Table I: Hyperfine-Shifted ^{1}H NMR Signals of Various Oxidized HiPIPs[a]

HiPIP [$E_{m,7}$ (mV)][b]	peak	chemical shift (ppm)	T_1 (ms)[c]	assignment
E. halophila I (120)	a	92.1	4.3	C_β-H of cysteinyl ligands
	b	46.8	2.5	C_β-H of cysteinyl ligands
	c	42.3	2.5	C_β-H of cysteinyl ligands
	d	29.0	2.5	C_β-H of cysteinyl ligands
	e	15.6	32.6	aromatic ring protons
	a′	−20.8	7.2	aromatic ring protons
	b′	−26.3	25.9	C_α-H of cysteinyl ligand
E. halophila II (50)	a	93.8	4.3	C_β-H of cysteinyl ligands
	b	57.8	2.5	C_β-H of cysteinyl ligands
	c	48.2	2.5	C_β-H of cysteinyl ligands
	a′	−13.2	11.5	aromatic ring protons
	b′	−16.8	17.3	aromatic ring protons
	c′	−20.1	7.2	aromatic ring protons
	d′	−23.5	25.9	C_α-H of cysteinyl ligand
E. vacuolata I (260)	a	101.4	*d*	C_β-H of cysteinyl ligands
	b	32.5	*d*	C_β-H of cysteinyl ligands
	c	30.1	*d*	C_β-H of cysteinyl ligands
	d	26.1	*d*	aromatic ring protons
	e	25.1	*d*	aromatic ring protons
	f	23.2	*d*	aromatic ring protons
	g	20.8	*d*	aromatic ring protons
	a′	−12.1	*d*	aromatic ring protons
	b′	−25.5	*d*	C_α-H of cysteinyl ligand
E. vacuolata II (150)	a	104.8	4.3	C_β-H of cysteinyl ligands
	b	32.5	4.3	C_β-H of cysteinyl ligands
	c	29.8	4.3	C_β-H of cysteinyl ligands
	d	25.2	25.9	aromatic ring protons
	e	23.9	7.2	aromatic ring protons
	f	22.8	7.2	aromatic ring protons
	a′	−15.9	7.2	aromatic ring protons
	b′	−25.5	25.9	C_α-H of cysteinyl ligand

[a] All data are reported at 23 °C, pH 7.0. [b] Midpoint redox potential at 25 °C, pH 7.0 (Meyer et al., 1983). [c] Estimated error ca. ±12%. [d] Not measured.

are sensitive, not only to the electronic structure of the active site (Phillips et al., 1970) but also to protein–active site interactions such as ionization of a histidine residue (Nettesheim et al., 1983). Since the longitudinal relaxation of these resonances is dominated by the iron-induced dipolar mechanism, structural information may be obtained on the basis of the r^{-6} dependence of the relative relaxation rate T_1^{-1} where r is the internuclear distance between the proton and the iron center (Swift, 1973).

We present herein the results of a comparative ^{1}H NMR study of *Ectothiorhodospira halophila* HiPIPs I and II and *Ectothiorhodospira vacuolata* HiPIPs I and II in their oxidized and reduced states. These four proteins exhibit quite different midpoint redox potentials (Table I) despite the fact that each pair of proteins from the same species shows more than 60% sequence identity (Przysiecki et al., 1985). Consideration of chemical shift, T_1 data, and Curie behavior of hyperfine-shifted signals in the spectra of all four oxidized HiPIPs led to their assignments to protons of the iron ligands: three to four of the cysteinyl C_β-H protons resonate downfield (about 30–100 ppm), and a C_α-H proton resonates upfield (about −25 ppm). The hyperfine shifts are consistent with a π-spin-transfer mechanism (Horrocks, 1973). Other hyperfine-shifted peaks were assigned to aromatic residues located at the active site on the basis of the anomalous temperature dependence of their chemical shifts. NMR studies of synthetic analogues of iron–sulfur clusters of the 4Fe-4S type (Holm et al., 1974; Que et al., 1974; Reynolds et al., 1978) have shown that the observed isotropic shifts in these systems are dominantly contact in origin. We propose that π–π interactions between the aromatic residues and sulfur atoms of the active site account for the large magnitude of the hyperfine shifts of aromatic groups. Hyperfine-shifted peaks present in spectra of the proteins dissolved in water but not in ^2H_2O have been assigned to exchange-labile protons at the active site. These protons most likely are hydrogen-bonded to the iron–sulfur cluster. The midpoint redox potential of HiPIP appears to be modulated both by hydrogen-bonding interactions and by aromatic π–π interactions involving the iron–sulfur cluster.

Materials and Methods

Protein Samples. HiPIPs from the bacteria *E. halophila* and *E. vacuolata* were isolated and purified according to the procedures of Bartsch (1978) and Meyer (1985) as described by Przysiecki et al. (1985). Purity indices for the oxidized state of these proteins, $A_{ox}^{290}/A_{ox}^{480}$, ranged from 1.9 to 2.2. The oxidation–reduction potentials of these HiPIPs were reported by Meyer et al. (1983). The proteins were lyophilized initially from solutions containing potassium phosphate buffer at pH 7.0. A typical NMR sample was prepared by dissolving about 2 mg of the lyophilized protein in 99.9% ^2H_2O containing 0.2 M KCl. The sample contained ~50 mM phosphate. About 1 equiv of solid potassium ferricyanide (one crystal) was added to produce an oxidized sample, and about 2 equiv of solid sodium dithionite (a few crystals) was added to produce a reduced sample. The pH of the solution was adjusted, if necessary, to the desired value with 0.2 M KO^{2}H or 0.2 M ^{2}HCl. The reported pH values were uncorrected for the isotope effect. Both the oxidized and the reduced samples were stable over the course of the NMR experiments. For the purpose of locating exchangeable protons, samples were prepared similarly, but in a solvent mixture containing 90% H_2O and 10% ^2H_2O (by volume).

NMR Spectroscopy. NMR spectra were obtained with a Nicolet NT-200 (200 MHz ^{1}H NMR) instrument. A simple 90° pulse (6 μs) was used with a spectral width of ±25 000 Hz over 8192 data points. The recycling time was about 0.6 s. The water signal was suppressed by a presaturation pulse (500 ms) from the decoupler. About 10 000 transients were coadded and Fourier-transformed to obtain a spectrum of

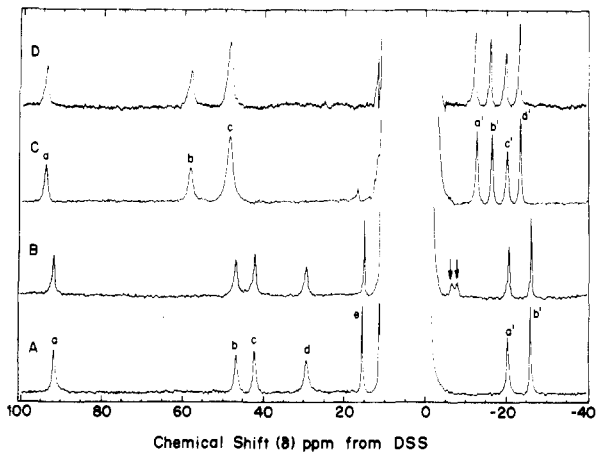

FIGURE 1: The 200-MHz ^1H NMR spectra of oxidized *E. halophila* HiPIPs at 23 °C, pH 7.0. The diamagnetic region, 0–10 ppm, has been zeroed out. (A) HiPIP I in ^2H_2O; (B) HiPIP I in H_2O; (C) HiPIP II in ^2H_2O; (D) HiPIP II in H_2O. The hyperfine-shifted solvent-exchangeable protons are identified with arrows.

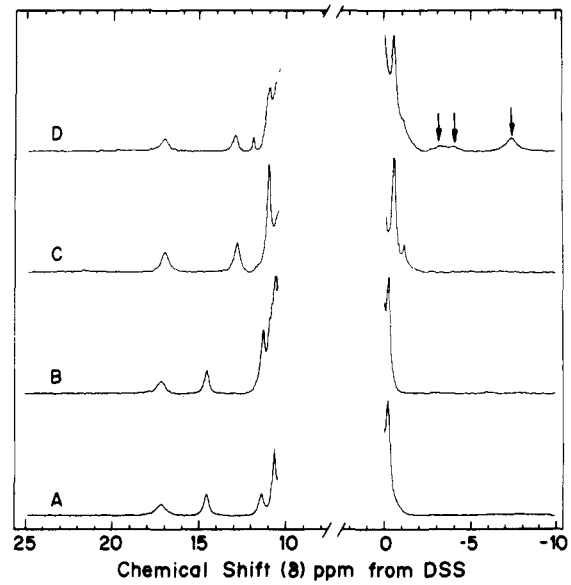

FIGURE 2: The 200-MHz ^1H NMR spectra of reduced *E. halophila* HiPIPs at 23 °C, pH 7.0. The diamagnetic region, 0–10 ppm, has been zeroed out. (A) HiPIP I in ^2H_2O; (B) HiPIP I in H_2O; (C) HiPIP II in ^2H_2O; (D) HiPIP II in H_2O. The hyperfine-shifted labile protons are identified with arrows. The resonance occurring at ~11 ppm in (D) corresponds to a solvent-labile proton located far from the iron–sulfur cluster, as indicated by its narrow line width. This proton is considered to have neglible effect on the stability of the cluster.

adequate signal to noise. All the spectra were base line corrected by using the subroutines available on the Nicolet 1180 data processing system. For the oxidized and reduced samples, the chemical shifts were referenced by assigning to the residual water signal in the spectra a value of 4.78 ppm relative to sodium 4,4-dimethyl-4-silapentane-1-sulfonate (DSS) at 23 °C. Correction was made (–0.05 ppm/5 °C) to the chemical shift of the residual water signal, when variable-temperature NMR studies were performed. In these studies, the probe temperature was varied and maintained by computer control. The spin–lattice relaxation times (T_1) were determined by using the standard inversion recovery sequence, $180°-\tau-90°$ (Vold et al., 1968), with the 180° pulse replaced by a composite $90_x240_y90_x$ pulse (Freeman et al., 1980).

RESULTS

The 200-MHz ^1H NMR spectra of oxidized *E. halophila* HiPIPs I and II in ^2H_2O and in H_2O at 23 °C, pH 7.0, are compared in Figure 1. The diamagnetic region, 0–10 ppm, is off scale and not shown. Peaks that are present in H_2O but not in ^2H_2O correspond to moderately slowly exchangeable protons. Protons that exchange rapidly with the solvent (lifetimes comparable to their longitudinal relaxation times, which are expected to be of the order of milliseconds) would have been cross-saturated by the water presaturation pulse. Protons that have exchange lifetimes greater than several hours would give rise to peaks in both spectra. Moderately slowly exchanging protons may correspond to hydrogen-bonded groups. Two such peaks in the spectrum of *E. halophila* HiPIP I (Figure 1B) suggest the presence of at least two hydrogen bonds involving the iron–sulfur cluster (peaks identified by arrows). These peaks appear to possess fractional intensities, probably because of saturation transfer from the irradiated water. Corresponding peaks are not present in the spectrum of oxidized *E. halophila* HiPIP II in H_2O (Figure 1D). The hyperfine shift patterns of nonexchangeable protons observed for the two proteins also differ: *E. halophila* HiPIP II exhibited four upfield peaks of unit proton intensity (Figure 1C), whereas the upfield spectrum of *E. halophila* HiPIP I (Figure 1A) reveals only two such peaks. These hyperfine-shifted peaks probably originate from the coordinating cysteinyl ligands or other residues very close to the iron–sulfur cluster.

Figure 2 presents the hyperfine-shifted regions of the 200-MHz ^1H NMR spectra of reduced *E. halophila* HiPIPs I and II in ^2H_2O (spectra A and C, respectively) and in H_2O (spectra B and D, respectively) at 23 °C, pH 7.0. The hyperfine shift patterns observed for these two proteins closely resemble each other. Since spin pairing leads to quenching of paramagnetism in reduced HiPIPs (Phillips et al., 1970), the spread of hyperfine shifts is only about 20 ppm. As a result, the sensitivity of the chemical shifts of the peaks to structural variations at the active site is decreased. Therefore, beyond noting the number of peaks and their exchange properties, we have not undertaken a detailed analysis of the ^1H NMR spectra of the reduced proteins. Our main interest here is confined to the hyperfine-shifted exchange-labile protons at the active site whose resonances are identified with arrows (Figure 2D). Reduced *E. halophila* HiPIP II appears to have at least three hydrogen-bonded protons at the active center. By contrast, the spectrum of reduced *E. halophila* HiPIP I reveals no labile proton resonances in the corresponding region of the spectrum (Figure 2B). The resonance at ~11 ppm in Figure 2D corresponds to a solvent-labile proton located far from the cluster, as revealed by its narrow linewidth. Such protons are unlikely to experience a hyperfine shift contribution and, hence, are not taken into account in the present study.

Figure 3 presents the 200-MHz ^1H NMR spectra of oxidized *E. vacuolata* HiPIPs I and II in ^2H_2O (spectra A and C, respectively) and in H_2O (spectra B and D, respectively) at 23 °C, pH 7.0. Only the regions containing the hyperfine-shifted resonances are shown. The hyperfine shift patterns from nonexchangeable protons of the two proteins closely resemble one another (Figure 3A,C, oxidized; Figure 4A,C, reduced), suggesting that the microenvironments of the active site of these two proteins are more similar to each other than those of the two *E. halophila* isozymes. However, the hyperfine-shifted resonances from exchange-labile protons show clear differences. Two such resonances are observed in the high-field spectrum of oxidized *E. vacuolata* HiPIP II (arrows in Figure 3D) but not *E. vacuolata* HiPIP I (Figure 3C). On the other hand, the high-field spectrum of reduced *E. va-*

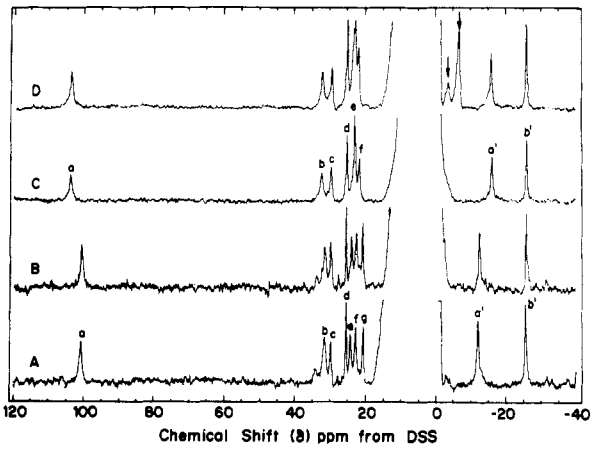

FIGURE 3: The 200-MHz ^{1}H NMR spectra of oxidized *E. vacuolata* HiPIPs at 23 °C, pH 7.0. The diamagnetic region, 0–10 ppm, has been zeroed out. (A) HiPIP I in ^2H_2O; (B) HiPIP I in H_2O; (C) HiPIP II in ^2H_2O; (D) HiPIP II in H_2O. The hyperfine-shifted labile protons are identified with arrows.

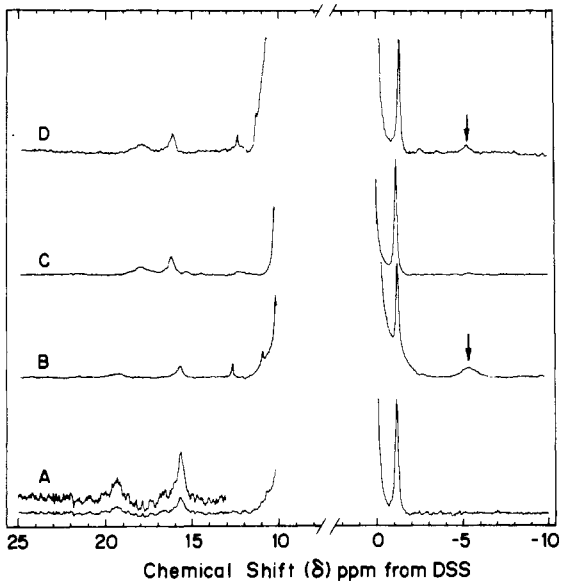

FIGURE 4: The 200-MHz ^{1}H NMR spectra of reduced *E. vacuolata* HiPIPs at 23 °C, pH 7.0. The diamagnetic region, 0–10 ppm, has been zeroed out. (A) HiPIP I in ^2H_2O; (B) HiPIP I in H_2O; (C) HiPIP II in ^2H_2O; (D) HiPIP II in H_2O. The hyperfine-shifted solvent-exchangeable protons are identified with arrows. The resonance found at ~12.5 ppm in (B) and (D) arises from a labile proton far removed from the iron–sulfur cluster, as revealed by its narrow line width. Therefore, it is considered to have little effect on the cluster stability.

cuolata HiPIP I (Figure 4B) shows at least one hyperfine-shifted exchange-labile proton near −5 ppm. A similar peak may be present in the spectrum of reduced *E. vacuolata* HiPIP II (Figure 4D). A peak of comparatively narrow line width is located at ~12.5 ppm in the spectra of both the reduced proteins in H_2O. Since the peak is sharp and not hyperfine shifted, it appears to correspond to an exchangeable proton located at a distance from the iron–sulfur cluster. Hence, it is unlikely to influence cluster stability.

Figure 5 is a Curie plot of the temperature dependence of the chemical shifts of the hyperfine-shifted resonances of oxidized *E. halophila* HiPIPs I and II. The hyperfine spectra of *E. vacuolata* HiPIPs I and II closely resemble one another at different temperatures, and the temperature dependence of the hyperfine-shifted resonances of the latter alone is illustrated in Figure 6. The intercept at $T^{-1} = 0$ is given within parentheses for each resonance that shows linear behavior. While most of the peaks obey the Curie law, some peaks in the spectra of *E. halophila* HiPIPs I and II as well as *E. vacuolata* HiPIPs I and II show either anti-Curie behavior, in the form of increasing shift with increasing temperature, or non-Curie behavior, in the form of curvature (La Mar, 1979).

Partially relaxed spectra showing the longitudinal relaxation behavior of various hyperfine-shifted peaks of oxidized *E. halophila* HiPIP II are shown in Figure 7. Similar results (not shown) were obtained with the other proteins. The experimental spin–lattice relaxation times for the hyperfine-shifted peaks of oxidized HiPIPs are collected in Table I.

Discussion

Assignments. It has been proposed recently (Nettesheim et al., 1983) that the presence of high- and low-field hyperfine-shifted resonances in the spectrum of an oxidized iron–sulfur protein may be diagnostic for HiPIP. Since the four proteins under investigation here have some of the high- and low-field hyperfine-shifted resonances previously found for *C. vinosum* and *R. gelatinosa* HiPIPs, this simple generalization appears to be partially correct. We confine ourselves to assignments of the hyperfine-shifted resonances in spectra of the oxidized proteins only. A combination of chemical shift, T_1 data, and temperature-dependent behavior of various resonances was employed to deduce the assignments. In principle, at least 12 hyperfine-shifted resonances corresponding to the four cysteinyl ligands (two β- and one α-proton for each) are to be expected. However, delocalization of the unpaired spin of the iron into the ligands is not necessarily uniform (La Mar, 1973), and consequently, some of these resonances may not be shifted far outside their normal diamagnetic positions. Examination of the longitudinal relaxation data in Table I reveals that the far low-field shifted peaks a–c (and d in the case of *E. halophila* HiPIP I) each relax much more efficiently than the high field ones, a′ and b′ (and c′ and d′ in the case of *E. halophila* HiPIP II). Particularly informative is the fact that the most downfield-shifted signal in all the four proteins studied (peak a) relaxes faster than any of the upfield peaks. This suggests that peak a arises from one of the C_β-H protons of a cysteinyl ligand because it is expected to have the closest proximity to the unpaired spin of the iron–sulfur cluster (Carter et al., 1974). The large magnitude of the observed hyperfine shift supports this assignment. If peak a corresponds to a C_β-H, then the other seven C_β-H peaks should also be shifted downfield. Thus, resonances b and c (and d in the case of *E. halophila* HiPIP I) are assigned to other cysteine C_β-H protons. Since the β-protons of the cysteinyl ligand are at an odd number of chemical bonds distant from the α-protons, we expect a reversal in the sign of their coupling constant compared to that of the α-protons, leading to a downfield contact shift. This is in agreement with the assignments made here.

At this stage we cannot assign these resonances to particular cysteines in the sequence. However, we suggest that each of the above peaks belongs to one of the two β-protons of the four different cysteinyl ligands.[2] The other stereotrophic proton of each of the cysteinyl ligands is not visible in the extreme low-field region, perhaps because of negligible overlap of its molecular orbital with the one containing the unpaired spin. The C_β-H_2 protons of the cysteines, because of their fixed

[2] Steady-state NOE experiments revealed no intensity changes for these resonances in the difference spectra when one of them was saturated, although magnetization transfer was observed among the upfield-shifted resonances (R. Krishnamoorthi, J. L. Markley, and M. A. Cusanovich, unpublished results).

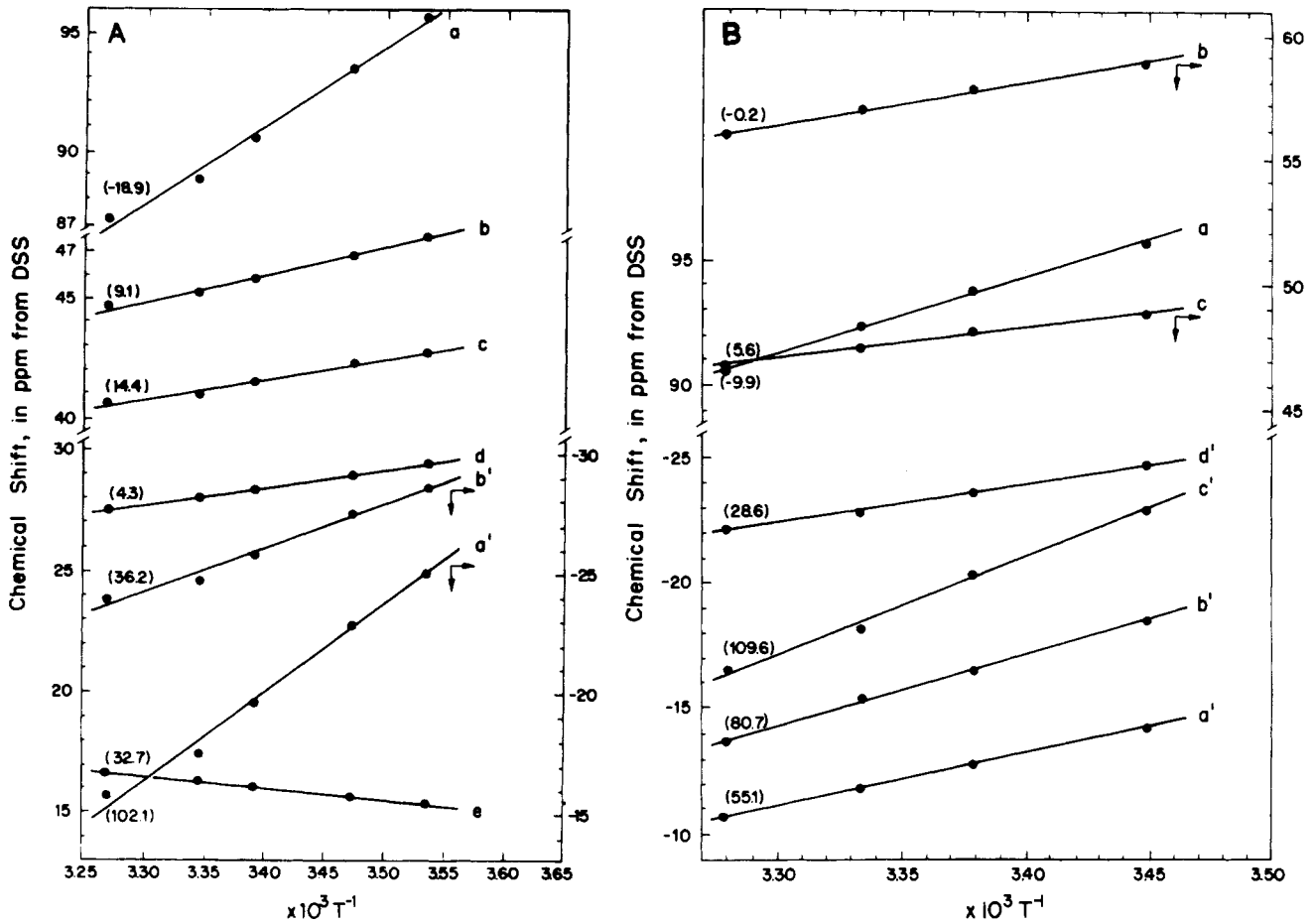

FIGURE 5: Curie plot for various hyperfine-shifted resonances of oxidized *E. halophila* HiPIPs: (A) HiPIP I; (B) HiPIP II. The apparent intercepts at $T^{-1} = 0$ are given within parentheses at the left of each set of data points that fall on straight lines.

geometry, probably sense spin densities on the adjacent sulfur atoms differentially. This is consistent with the conclusion based on the study of iron–sulfur cluster model compounds (Holm et al., 1974; Que et al., 1974; Reynolds et al., 1978) that the observed isotropic shift is contact in origin. A dipolar shift mechanism would be expected to shift the other C_β-H protons at least beyond the diagmagnetic region, if not by the same amount.

We would like to emphasize the finding that the hyperfine-shifted exchange-labile proton resonances are located only in the upfield region. Since dipolar contribution to the observed isotropic shift is expected to be negligible, the observed hyperfine shift of solvent-exchangeable HiPIP protons probably arises mainly from direct hydrogen bonding to the cluster, in particular involving the π-orbitals of the sulfur. Such an interaction would lead to an upfield contact shift (Horrocks, 1973).

Further assignments are proposed by considering the temperature dependence of the hyperfine-shifted resonances. It is clear from Figure 5 that resonance e of *E. halophila* HiPIP I shows anti-Curie behavior, while all the other resonances show the expected Curie behavior of moving toward their diamagnetic positions with increasing temperature. Anti-Curie behavior can result from any additional interaction that changes the spin-density distribution with temperature (La Mar, 1979). The T_1 value of resonance e (32.6 ms) suggests that this peak arises from a group near the iron. In addition, the peak shows a contact shift of 16 ppm. These observations can be rationalized by assigning this resonance to an aromatic residue in contact with the π-system of the iron–sulfur cluster. From the X-ray coordinates of *C. vinosum* HiPIP (Carter et al., 1974), Morgan et al. (1978) have identified a number of aromatic residues that are close enough to the sulfur atoms of the iron–sulfur cluster so as to permit π–π interactions. It is likely that an increase in temperature in this situation causes a change in the local conformation of the protein such that the π–π interaction is strengthened with a concomitant increase in the contact shift. Since the other resonances of *E. halophila* HiPIP I do not show similar temperature behavior, a general cause, such as populating a more paramagnetic electronic excited state of the iron–sulfur cluster with increased temperature, is ruled out.

We next consider the intercept values of the hyperfine-shifted peaks of oxidized *E. halophila* HiPIPs I and II. Resonances e and a′ of *E. halophila* HiPIP I and resonances a′–c′ of *E. halophila* HiPIP II all show abnormal intercepts. If a hyperfine-shifted resonance strictly obeys the Curie law, then the intercept should be the normal diamagnetic shift expected of the resonance (La Mar, 1979). Clearly, all the above-mentioned resonances exhibit abnormal temperature-dependent behavior. Particularly worth mentioning are the extrapolated chemical shift values of 102.1 ppm determined for the upfield-shifted resonance a′ of *E. halophila* HiPIP I and 109.6 ppm determined for the upfield-shifted resonance c′ of *E. halophila* HiPIP II. These values imply that the hyperfine shift in these cases does not result from the normal orbital overlap expected of covalently bonded systems but mainly from another type of interaction that leads to a temperature dependence in the magnitude of the unpaired spin transfer. A π–π interaction between the iron–sulfur cluster and the aromatic residue would possess the above properties. Similar interactions have been known to operate in heme

Table II: Cluster Packing Residues in *E. halophila* and *E. vacuolata* HiPIPs I and II[a]

HiPIP	amino acid position[b]											
	17	19	48	49	60	65	66	68	71	75	76	80
C. vinosum	L	Y	F	M	W	L	F	G	I	G	W	W
E. halophila I	H	Y	F	W	W	*c*	H	D	V[d]	*e*	W	Y
E. halophila II	H	Y	F	W	W	*c*	H	D	V[f]	*g*	W	Y
E. vacuolata I	L	Y	L	Y	W	V	F	N	V	G	W	Y
E. vacuolata II	L	Y	L	Y	W	V	F	G	V	G	W	W

[a] Przysiecki et al. (1985). The amino acid sequences of *E. halophila* HiPIPs are the unpublished data of Tedro, Meyer, and Kamen. The amino acid sequences of *E. vacuolata* HiPIPs are the unpublished data of Ambler, Meyer, Fischer, and Kamen. [b] Based on the X-ray crystal structure data of *C. vinosum* HiPIP (Carter et al., 1974). [c] Deletion. [d] Insertion at Gln-70a. [e] Insertion at Lys^{73a}-Ala^{73b}. [f] Insertion at Asp-70a. [g] Insertion at Arg^{73a}-Gly^{73b}.

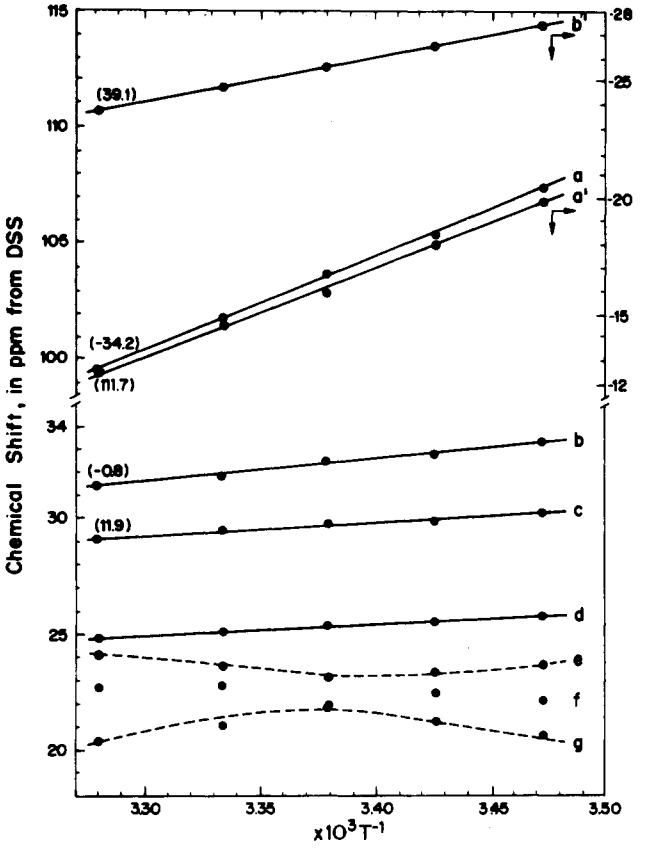

FIGURE 6: Curie plot for various hyperfine-shifted peaks of oxidized *E. vacuolata* HiPIP II. The apparent intercepts at $T^{-1} = 0$ are given within parentheses at the left for those sets of data points that fall on straight lines.

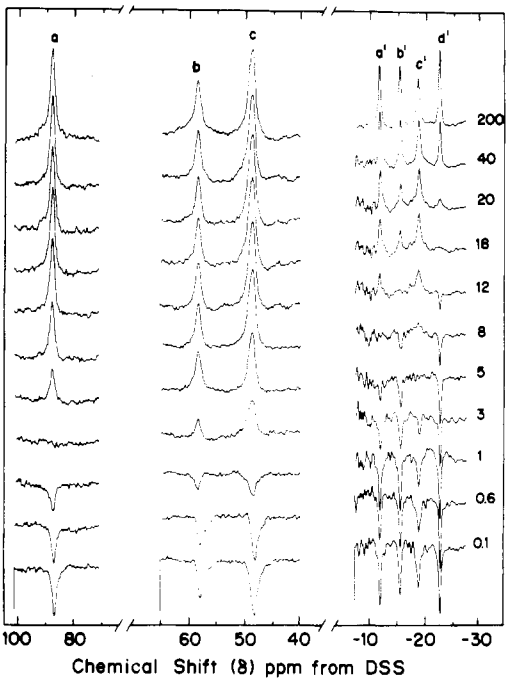

FIGURE 7: Partially relaxed 200-MHz ^{1}H NMR spectra of oxidized *E. halophila* HiPIP II, pH 7.0, 25 °C. The delay times, τ (ms), in the conventional 180°–τ–90° pulse sequence used (Vold et al., 1968) are given at the end of each trace.

proteins (Rousseau et al., 1982; Krishnamoorthi & La Mar, 1984). A major dipolar contribution to the observed isotropic shift is ruled out as the cause, since some of the hyperfine-shifted resonances, including the farthest downfield shifted peak, show normal behavior.[3]

The X-ray crystal structure data of *C. vinosum* HiPIP (Carter et al., 1974) indicate that several aromatic residues including tyrosine-19, phenylalanine-48, tryptophan-60, phenylalanine-66, tryptophan-76, and tryptophan-80 pack the iron–sulfur cluster within a distance of <5.5 Å. Of these, tyrosine-19 has been implicated in the electron-transfer step, because it is about 4.1 Å from the active center (Carter et al., 1974; Carter, 1977b). The amino acid residues in the corresponding positions in the cluster binding segments of *E. halophila* HiPIPs I and II as well as *E. vacuolata* HiPIPs I and II have been identified (Table II) on the basis of sequence homology (Przysiecki et al., 1985) and the X-ray crystal structure data of *C. vinosum* HiPIP (Carter et al., 1974). The T_1 value of resonances a′ (7.2 ms) of *E. halophila* HiPIP I (Figure 1A) and c′ (7.2 ms) of *E. halophila* HiPIP II (Figure 1C), which appear to arise from the same group, indicate that this proton must be at least as close as is the cysteinyl C_α-H proton to the iron–sulfur cluster.[4] Therefore, we assign this peak to a ring proton of tyrosine-19 in each case. Since the π–π overlap involves a plane perpendicular to the aromatic plane, it is likely that only one of the carbon atoms of the aromatic ring participates in this type of interaction. Similar localized interactions involving π-orbitals have been observed in simple organic compounds (Szent-Gyorgyi et al., 1961). In the absence of X-ray crystal structure data for these proteins, specific assignments to other aromatics in the vicinity of the active site are not proposed.

[3] Extrapolation of data obtained in a narrow temperature range to an infinite temperature must be interpreted with caution. Different factors, such as a major dipolar shift contribution to the observed isotropic shift, zero field splitting, and the presence of residual antiferromagnetism, can cause anomalous temperature dependences of hyperfine-shifted resonances. In the present study, consideration of several properties of the various hyperfine-shifted resonances suggests that the postulated π–π interaction mechanism is not unreasonable.

[4] From the X-ray diffraction data of *C. vinosum* HiPIP (Carter et al., 1974), we calculated the distance between an inorganic sulfur atom of the cluster and the C_δ ring atom of tyrosine-19 to be 3.66 Å.

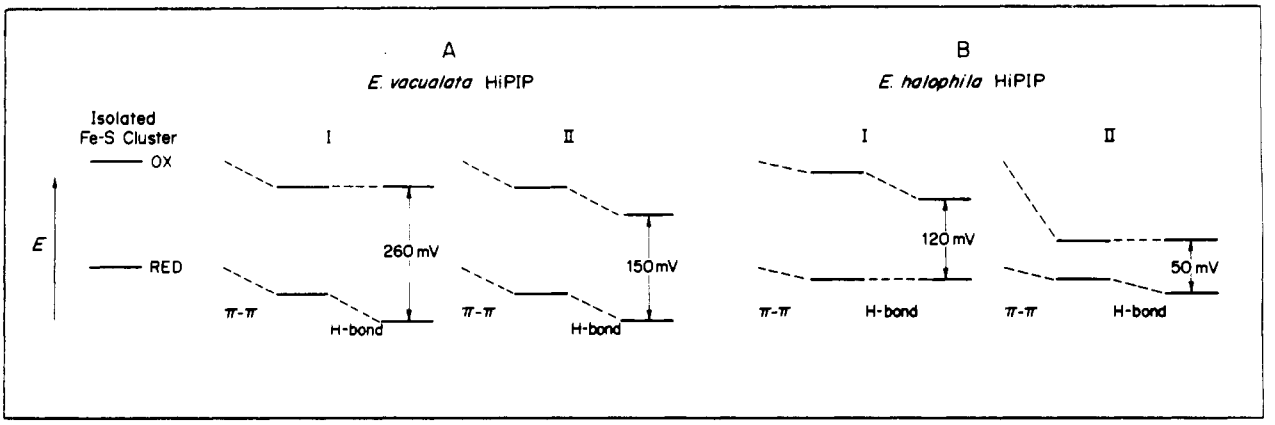

FIGURE 8: Schematic representation of the contribution of π–π and hydrogen-bonding interactions to the stability of the oxidized and reduced forms of the iron–sulfur cluster in various HiPIPs studied as deduced from ^{1}H NMR data: (A) *E. vacuolata* HiPIPs I and II; (B) *E. halophila* HiPIPs I and II.

Peaks b′ of *E. halophila* HiPIP I and d′ of *E. halophila* HiPIP II are assigned to the ligated cysteinyl C_α-H protons on the basis of their T_1 values and the near normal intercepts in the Curie plot. The inverse sixth power of the ratios of the T_1 values of b′ and a and of d′ and a (1.349) are in reasonable agreement with the values available from the X-ray crystal structure data of *C. vinosum* HiPIP (Carter et al., 1974) for the ratios of distances of the four ligated cysteinyl C_α and C_β atoms from the iron atoms of the cluster.[5] Other C_α-H protons apparently are not shifted outside the diamagnetic envelope; the spin distribution is nonuniform, as evidenced by the spread of the hyperfine shifts of the cysteinyl β-protons (Figure 1). We attribute the hyperfine shift of the α-protons to the effect of spin correlation (La Mar, 1973). Since the contact shift depends upon the angular overlap of the orbitals (La Mar, 1979), the decrease in magnitude observed for the α-proton suggests decreased overlap, accompanied by a smaller amount of π-spin transfer. Resonances a′ and b′ of *E. halophila* HiPIP II exhibit T_1 values of 11.5 and 17.3 ms (Table I) and intercept values of 55.1 and 80.7 ppm, respectively (Figure 5B). These NMR characteristics suggest their assignments to interacting aromatics within 4.2 Å from the iron–sulfur cluster. The X-ray crystal structure data of *C. vinosum* HiPIP show that the aromatic ring of tyrosine-19 and the cysteine-43 sulfur atom are within 4.1 Å of each other (Carter et al., 1974). Therefore, peak a′ is assigned to a tyrosine-19 ring proton. Similarly, peaks a′–c′ of *E. halophila* HiPIP II are assigned to aromatic residues as supported by their intercept values (Figure 5B), chemical shifts, and T_1 values (Table I).

The overall hyperfine shift patterns of oxidized *E. vacuolata* HiPIPs I and II (Figure 3) are found to be very similar; consequently, we conclude that there is no major structural difference between these two proteins at the active site region. We adopt similar lines of reasoning and arguments as before for assigning these peaks. Thus, on the basis of their shorter T_1 values (Table I) and near-normal intercepts in the Curie plot (Figure 6), resonances a–c are assigned to the C_β-H protons and b′ to a C_α-H proton of the cysteinyl ligands. Resonance a′ shows an intercept of 111.7 ppm in the Curie plot and has a T_1 of 7.2 ms. We assign this peak to a tyrosine-19 ring proton adjacent to the iron–sulfur cluster. The fact that one of the upfield-shifted resonances in the spectra of all the four HiPIPs studied shows a similar chemical shift, T_1, and temperature dependence strongly suggests that it be assigned to a highly conserved residue, which retains its geometrical position relative to the iron–sulfur cluster in these proteins. Its assignment to tyrosine-19 is consistent with the fact that this residue is invariant in all the above proteins (Table II). It is also to be noted that the spectral properties (chemical shift, longitudinal relaxation, and temperature dependence) of the upfield-shifted cysteine C_α-H proton of each HiPIP studied here are similar.

Resonances d–g of *E. vacuolata* HiPIP I (Figure 3) show curvature in the Curie plot (Figure 6). The T_1 data of these peaks (Table I) indicate their proximity to the iron (within 5 Å). These observations qualify these peaks to be assigned to aromatic residues in the active site region (Table II). The non-Curie behavior of these resonance is probably due to temperature-modulated π–π interactions between these residues and the iron–sulfur cluster. It is likely that the presence of a heteroatom connected to the π-system (as in tryptophan and tyrosine) is responsible for the change in sign of the observed contact shift. The relatively smaller magnitudes and spread of the hyperfine shifts of the above peaks are consistent with this assignment.

Sources of Modulation of the Redox Potential of HiPIP. The location of labile protons at the active site sheds some light on the structural details of the active site of the HiPIPs studied. It has been shown theoretically (Sheridan et al., 1981, 1984) that hydrogen bonds between the iron–sulfur cluster and the polypeptide chain can influence the stability and, hence, the redox potential. The midpoint redox potential measured for any protein is simply a measure of the difference in the stability of the oxidized and reduced states. Modulation of the redox potential of a given kind of iron–sulfur cluster will result from differential stabilization of the iron–sulfur cluster in the two states by the surrounding polypeptide chain. If the oxidized cluster is more stabilized than the reduced, the redox potential will decrease; alternatively, if the reduced cluster is stabilized more than the oxidized, the redox potential will increase.

Different interactions may be expected to stabilize the iron–sulfur cluster such as π–π interactions or hydrogen bonding. One pair of HiPIPs studied (*E. vacuolata* I and II) appears to have similar π–π interactions as deduced from conservation of the nonexchangeable hyperfine-shifted peak pattern (Figures 3 and 4). These proteins do differ, however, in the number of hydrogen bonds to the iron–sulfur cluster, as evidenced by differences in the patterns of exchangeable hyperfine-shifted peaks. The spectra suggest that oxidized *E. vacuolata* HiPIP II has three hydrogen bonds that are not present in oxidized HiPIP I from the same species. The number of hydrogen bonds in the reduced forms of these

[5] The following ratios were obtained for the cysteinyl ligands: 1.203 (Cys-43), 1.428 (Cys-46), 1.345 (Cys-63), and 1.380 (Cys-77).

proteins appear similar.[6] Thus, the proposed hydrogen bonds explain qualitatively the observed redox potentials (Meyer et al., 1983) (*E. vacuolata* HiPIP I, 260 mV; *E. vacuolata* HiPIP II, 150 mV) as shown schematically in Figure 8A.

The other pair of HiPIPs studied (*E. halophila* I and II) exhibit differences in both $\pi-\pi$ interactions and numbers of hydrogen bonds to the iron–sulfur cluster. Provided that signals from all relevant hydrogen bonds and $\pi-\pi$ interactions have been resolved, we can attempt to rationalize, on the basis of the spectra data, the observed difference in redox potential of these proteins (*E. halophila* HiPIP I, 120 mV; *E. halophila* HiPIP II, 50 mV). Clearly, the difference in hydrogen bonds predicts preferential stabilization of the oxidized form of *E. halophila* HiPIP I and the reduced form of *E. halophila* HiPIP II. By contrast, the $\pi-\pi$ interaction stabilizes only the oxidized form of *E. halophila* HiPIP II. The observed hydrogen bonding and $\pi-\pi$ interactions oppose one another so that to explain the difference in redox potential one must postulate that the magnitude of $\pi-\pi$ stabilization is much larger than hydrogen-bond stabilization as shown schematically in Figure 8B.

Conclusions

In the ^{1}H NMR spectra of several oxidized HiPIPs it is found that a resolved cysteinyl C_β-H proton resonates far downfield ($\sim$100 ppm) and a C_α-H proton far upfield (ca. −25 ppm). This hyperfine shift pattern for the iron ligands provides evidence that the isotropic shift is dominantly contact in origin. In highly homologous proteins, the number and position of hyperfine shifted peaks are indicative of structural details of the active site microenvironment. Hydrogen-bonding interactions as well as aromatic $\pi-\pi$ interactions involving the iron–sulfur cluster exist in HiPIP. These interactions apparently modulate the stability of the protein in its two redox states and hence its redox potential.

Acknowledgments

We thank Dr. T.-M. Chan for suggesting this collaboration and for recording some preliminary NMR spectra.

References

Adman, E., Watenbough, K. D., & Jensen, L. H. (1975) *Proc. Natl. Acad. Sci. U.S.A. 72*, 4854–4858.

Bartsch, R. G. (1978) *Methods Enzymol. 53*, 329–340.

Carter, C. W., Jr. (1977a) in *Iron-Sulfur Proteins* (Lovenberg, W., Ed.) Vol. III, pp 157–204, Academic Press, New York.

Carter, C. W., Jr. (1977b) *J. Biol. Chem. 252*, 7802–7811.

Carter, C. W., Jr., Kraut, J., Freer, S. T., & Alden, R. A. (1974) *J. Biol. Chem. 249*, 6339–6346.

Freeman, R., Kempsell, S. P., & Levitt, M. H. (1980) *J. Magn. Reson. 38*, 453–479.

Fukumari, Y., & Yamanaka, T. (1979) *Curr. Microbiol. 3*, 117–120.

Holm, R. H., Phillips, W. D., Averill, B. A., Mayerle, J. J., & Herskovitz, T. (1974) *J. Am. Chem. Soc. 96*, 6042–6048.

Horrocks, W. D., Jr. (1973) in *NMR of Paramagnetic Molecules* (La Mar, G. N., Horrocks, W. D., Jr., & Holm, R. H., Eds.) pp 127–177, Academic Press, New York.

Krishnamoorthi, R., & La Mar, G. N. (1984) *Eur. J. Biochem. 138*, 135–140.

La Mar, G. N. (1973) in *NMR of Paramagnetic Molecules* (La Mar, G. N., Horrocks, W. D., Jr., & Holm, R. H., Eds.) pp 85–126, Academic Press, New York.

La Mar, G. N. (1979) in *Biological Applications of Magnetic Resonance* (Shulman, R. G., Ed.) pp 305–343, Academic Press, New York.

Laskowski, E. J., Frankel, R. B., Gillum, W. D., Papaefthymiou, G. L., Renaud, J., Ibers, J. A., & Holm, R. H. (1978) *J. Am. Chem. Soc. 100*, 5322–5337.

Meyer, T. E. (1985) *Biochim. Biophys. Acta 806*, 175–183.

Meyer, T. E., Przysiecki, C. T., Watkins, J. A., Bhattacharyya, A., Simondsen, R. P., Cusanovich, M. A., & Tollin, G. (1983) *Proc. Natl. Acad. Sci. U.S.A. 80*, 6740–6744.

Morgan, R. S., Tatsch, C. E., Gushard, R. H., McAdon, J. M., & Warme, P. K. (1978) *Int. J. Pept. Protein Res. 11*, 209–217.

Nettesheim, D. G., Meyer, T. E., Feinberg, B. A., & Otvos, J. D. (1983) *J. Biol. Chem. 258*, 8235–8239.

Phillips, W. D. (1973) in *NMR of Paramagnetic Molecules* (La Mar, G. N., Horrocks, W. D., Jr., & Holm, R. H., Eds.) pp 421–478, Academic Press, New York.

Phillips, W. D., & Poe, M. (1973) in *Iron-Sulfur Proteins* (Lovenberg, W., Ed.) Vol. II, pp 255–284, Academic Press, New York.

Phillips, W. D., Poe, M., McDonald, C. C., & Barsch, R. G. (1970) *Proc. Natl. Acad. Sci. U.S.A. 67*, 682–687.

Przysiecki, C. T., Meyer, T. E., & Cusanovich, M. A. (1985) *Biochemistry 24*, 2542–2549.

Que, L., Jr., Anglin, J. R., Bobrik, M. A., Davison, A., & Holm, R. H. (1974) *J. Am. Chem. Soc. 96*, 6042–6048.

Reynolds, J. G., Laskowski, E. J., & Holm, R. H. (1978) *J. Am. Chem. Soc. 100*, 5315–5322.

Roussueau, D. L., Shelnutt, J. A., Ondrias, M. R., Freidman, J. M., Henry, E. R., & Simon, S. R. (1982) in *Hemoglobin and Oxygen Binding* (Ho, C., Ed.) pp 223–229, Elsevier/North-Holland, New York.

Sheridan, R. P., & Allen, L. C. (1980) *Chem. Phys. Lett. 69*, 600–604.

Sheridan, R. P., Allen, L. C., & Carter, C. W., Jr. (1981) *J. Biol. Chem. 256*, 5052–5057.

Sheridan, R. P., Knight, E. T., & Allen, L. C. (1984) *Biopolymers 23*, 195–200.

Swift, T. J. (1973) in *NMR of Paramagnetic Molecules* (La Mar, G. N., Horrocks, W. D., Jr., & Holm, R. H., Eds.) pp 53–83, Academic Press, New York.

Szent-Gyorgyi, A., Isenberg, & McLaughlin, J. (1961) *Proc. Natl. Acad. Sci. U.S.A. 47*, 1089–1093.

Vold, R. L., Waugh, J. S., Klein, M. P., & Phelps, D. E. (1968) *J. Chem. Phys. 48*, 3831–3832.

[6] The evidence for a conserved hydrogen bond to the iron–sulfur cluster of reduced *E. vacuolata* HiPIPs I and II is tenuous since the peak around −5 ppm in spectrum D of Figure 4 is of low intensity. If this peak is an artifact and the hydrogen bond is present in HiPIP I but not in HiPIP II, this would lead only to a larger predicted decrease in the redox potential of *E. vacuolata* HiPIP II compared to that of *E. vacuolata* HiPIP I.